Journal of Zhejiang University-SCIENCE B (Biomedicine & Biotechnology)
ISSN 1673-1581 (Print); ISSN 1862-1783 (Online)
www.zju.edu.cn/jzus; www.springerlink.com
E-mail: jzus@zju.edu.cn

Endostatin inhibits hypertrophic scarring in a rabbit ear model*

Hai-tao REN[1], Hang HU[1], Yuan LI[2], Hong-fei JIANG[3], Xin-lei HU[1], Chun-mao HAN[†‡1]

([1]*Department of Burns and Wound Center, the Second Affiliated Hospital, School of Medicine, Zhejiang University, Hangzhou 310009, China*)

([2]*Department of Ultrasound, Women's Hospital, School of Medicine, Zhejiang University, Hangzhou 310006, China*)

([3]*Assisted Reproduction Unit, Department of Obstetrics and Gynecology, Sir Run Run Shaw Hospital, School of Medicine, Zhejiang University, Hangzhou 310016, China*)

[†]E-mail: hanchunmao1@126.com

Received Mar. 14, 2012; Revision accepted Sept. 9, 2012; Crosschecked Jan. 3, 2013

Abstract: Objective: The present study was designed to use an in vivo rabbit ear scar model to investigate the efficacy of systemic administration of endostatin in inhibiting scar formation. Methods: Eight male New Zealand white rabbits were randomly assigned to two groups. Scar model was established by making six full skin defect wounds in each ear. For the intervention group, intraperitoneal injection of endostatin was performed each day after the wound healed (about 15 d post wounding). For the control group, equal volume of saline was injected. Thickness of scars in each group was measured by sliding caliper and the scar microcirculatory perfusion was assessed by laser Doppler flowmetry on Days 15, 21, 28, and 35 post wounding. Rabbits were euthanatized and their scars were harvested for histological and proteomic analyses on Day 35 post wounding. Results: Macroscopically, scars of the control group were thicker than those of the intervention group. Significant differences between the two groups were observed on Days 21 and 35 (p<0.05). Scar thickness, measured by scar elevation index (SEI) at Day 35 post wounding, was significantly reduced in the intervention group (1.09±0.19) compared with the controls (1.36±0.28). Microvessel density (MVD) observed in the intervention group (1.73±0.94) was significantly lower than that of the control group (5.63±1.78) on Day 35. The distribution of collagen fibers in scars treated with endostatin was relatively regular, while collagen fibers in untreated controls were thicker and showed disordered alignment. Western blot analysis showed that the expressions of type I collagen and Bcl-2 were depressed by injection of endostatin. Conclusions: Our results from the rabbit ear hypertrophic scar model indicate that systemic application of endostatin could inhibit local hypertrophic scar formation, possibly through reducing scar vascularization and angiogenesis. Our results indicated that endostatin may promote the apoptosis of endothelial cells and block their release of platelet-derived growth factor (PDGF) and fibroblast growth factor (FGF), thereby controlling collagen production by fibroblasts. Blood vessel-targeted treatment may be a promising strategy for scar therapy.

Key words: Endostatin, Hypertrophic scar, Systemic administration
doi:10.1631/jzus.B1200077 **Document code:** A **CLC number:** R644

1 Introduction

Hypertrophic scar (HS) formation is a common complication of wound healing, particularly after burn injuries. HSs are raised, red, rigid, and responsible for serious functional and cosmetic problems. The underlying mechanisms of scar formation are complicated, and the process may be affected by multiple factors.

Angiogenesis and vascularization are the important processes during wound healing. These events ensure abundant microvascular perfusion for the regeneration of the neo-tissue (Kirsner and Eaglstein, 1993). However, excessive angiogenesis and vascularization can lead to pathological HSs (Kischer, 1992). Microvascular abnormalities have been observed in pathological scars. Compared with

‡ Corresponding author

* Project supported by the National Natural Science Foundation of China (No. 81272120) and the Health Department of the Zhejiang Province (No. 2007B086), China

normal skin, such scars have vessels of greater density and diameter and blood flow is increased as measured by laser Doppler. This implies the presence of increased vascular density in HSs compared with normotrophic scars. Amadeu *et al*. (2003) have reported increased microvessel numbers in HSs. Thomas *et al*. (1994) confirmed that HSs have an increased vascular component. Ehrlich and Kelley (1992) also demonstrated increased blood flow in HSs. Thus, we propose that inhibition of the growth of excessive new blood vessels in the scar might be a promising new strategy for the suppression of HS formation.

Currently, surgical excision, intralesional injection of steroids, silicone, and laser are the most frequently used treatments for HSs (Leventhal *et al*., 2006). However, no single treatment appears to have the desired curative effect. As a result, new strategies for prevention of HSs are needed to avoid completely their formation. Antiangiogenic therapy may be used as an effective strategy in HS therapy. There have been some studies in the area of antiangiogenic therapy for HSs (Song *et al*., 2008a; 2008b; 2009); however, the antiangiogenic agents used in these reports are topically administered, which can lead to local pain and poor compliance.

Endostatin, the C-terminal fragment of collagen XVIII, has been clinically applied to suppress tumor growth and angiogenesis by inhibiting endothelial cell proliferation and migration (Song *et al*., 2009; Zheng, 2009). We propose that this anti-angiogenesis of endostatin may also be effective in scar-treatment.

The aim of this study was to investigate our hypothesis that endostatin may be successful in the therapeutic modulation of scar formation in vivo.

2 Materials and methods

2.1 HS model

Eight male adult New Zealand white rabbits weighing between 2.2 and 2.5 kg were used in this study. All animal handling procedures were approved by the Zhejiang University Animal Care and Use Committee. Animals were anaesthetized with 1% (10 g/L) pentobarbital sodium (1 mg/kg). Afterwards, the HS model was made following standardized protocol, as previously described (Morris *et al.*, 1997; Saulis *et al.*, 2002b). Six wounds were created down to bare cartilage on the ventral surface of each ear by means of a 7-mm punch biopsy at standardized locations (Tandara and Mustoe, 2008). An operating loupe was used to ensure removal of the epidermis, dermis, and perichondrium in each wound (Tandara and Mustoe, 2008). Hemostasis was then obtained by applying pressure with cotton balls.

2.2 Animal groups and drug administration

Eight rabbits were randomly assigned to either the intervention group or the control group such that each group had four members. Human recombinant endostatin (Endostar™, purchased from SIMCERE PHARMACEUTICAL Company, 15 mg/3 ml per dosage) was diluted with 47 ml physiological saline. Endostar™ solution was given to the intervention group rabbits by intraperitoneal injection every day from the Day 15 after operation when the wound had finished epithelialization. The dosage was calculated based on body surface area following the users' instructions for Endostar™. The animal body surface area calculation formula is $S=K\times W^{2/3}$ (S: surface area, K: constant, W: weight); for the rabbit K=10. A 2.5 kg rabbit has a body surface area of 0.2 m^2 ($S=10\times2\,500^{2/3}=1\,842$ $cm^2\approx0.2$ m^2), and 5 ml of Endostar™ solution containing 1.5 mg endostatin was injected each day.

2.3 Tissue preparation

On Day 35 post wounding, the rabbits of each group were sacrificed and the scars harvested. To prevent scar shrinkage in paraffin sections, the samples contained the rabbit ear full-thickness scar skin and the cartilage, the latter acting as a tissue pedestal. One half of each scar was fixed in 4% neutral-buffered formaldehyde, dehydrated, embedded in paraffin, cut in 4-mm sections, and stained with haematoxylin and eosin (H&E). The other half was frozen for Western blot analysis.

2.4 Microcirculation perfusion assessment

On Days 15, 21, 28, and 35 post wounding, scar microcirculatory perfusion was assessed by laser Doppler flowmetry (PeriFlux5000s, PF 5010 standard probe; Perimed, Stockholm, Sweden) according to the manufacturer's instructions as previously described (Song *et al.*, 2009). In short, a 1-mW laser source with

a wavelength of 780 nm was used, and the time duration was set at 60 s for each measurement spot in each scar. The output signal was analyzed using PSW 2.0 software, and the average value was obtained for a total of 96 scars at each time point of investigation.

2.5 Scar elevation index (SEI)

The degree of dermal hypertrophy of each scar was expressed as the SEI (Morris *et al.*, 1997; Tandara and Mustoe, 2008). This index is the ratio of the area of newly formed dermis of the scar to the area of surrounding normal dermis. An SEI value greater than 1.0 defines a hypertrophic dermis (Morris *et al.*, 1997; Marcus *et al.*, 2000; Saulis *et al.*, 2002a; Tandara and Mustoe, 2008).

2.6 Immunohistochemistry and microvessel density (MVD)

Specific immunochemical staining of endothelial cells was performed using a monoclonal antibody to CD34. Mouse-anti-rabbit-CD34 monoclonal antibody was purchased from Santa Cruz Biotechnology. In each scar, the total number of CD34 positive blood vessels was counted in five randomly chosen high power fields, which were distributed evenly inside the scar. The counts from the five fields (200×) were averaged and used for comparisons.

2.7 Collagen organization and cellularity of the dermis

The dermis was examined for collagen organization in a semi-quantitative manner in Masson trichrome-stained slides as described previously (Saulis *et al.*, 2002b; Tandara and Mustoe, 2008). The collagen organization was described by its alignment and thickness.

2.8 Western blot analysis

Western blot was performed using a previously described method (Kim *et al.*, 2007; 2011). Scar samples were lysed in solutions containing 250 mmol/L sucrose, 1 mmol/L ethylenediaminetetraacetic acid (EDTA), 0.1 mmol/L phenylmethylsulfonyl fluoride (PMSF), and 20 mmol/L potassium phosphate buffer at pH 7.6 with a homogenizer at 3000 r/min. Equal amounts of protein (50 mg/lane) were subjected to immunoblotting with the indicated antibodies. The antibodies used were type I collagen, Bcl-2, and β-actin (200 μg/ml, Santa Cruz Biotechnology, CA, USA). The bound horseradish peroxidase conjugated secondary antibody was detected using an enhanced chemiluminescence detection system (iNtRON Biotechnology, Korea). Protein expression levels were determined by analyzing the signals captured on the nitrocellulose membranes using an image analyzer (Las-3000, Fuji photo, Tokyo, Japan).

2.9 Statistical analysis

Each sample was evaluated twice at each time points using a calibrated eyepiece reticule. SPSS Version 18 (SPSS Inc.) was used for statistical analysis. Continuous variables are expressed as mean±standard deviation (SD). Enumeration data are expressed as percentages. A p-value of <0.05 was chosen to indicate statistical significance. We first checked the normality and homogeneity of the continuous variables, and then adopted an independent sample t-test or nonparametric independent sample test to analyze the differences between variables of both groups, depending on the distribution of the variables.

3 Results

3.1 Appearance of scars

Macroscopic view of scar samples was taken at each time point by digital camera (Fig. 1).

One week after complete healing (Day 21), the scars in the control group were severely congested and appeared purple and swollen (Fig. 1a). Since the perfusion of scars in the intervention group was dramatically depressed due to the injection of endostatin, these scars appeared pink and less swollen (Fig. 1b). Three weeks after healing, the intra scar microvascular perfusion in both groups had decreased, and the scars had become less red. However, scars in the control group were still thick, and had even become hardened (Fig. 1c), while scars in the intervention group were completely flat and had softened (Fig. 1d).

3.2 Thickness of scars in the rabbit ear

The thickness of scars in both groups was measured with a slide gauge (Table 1 and Fig. 2).

On Day 15 the scar thickness in both groups had peaked, and there was no significant difference

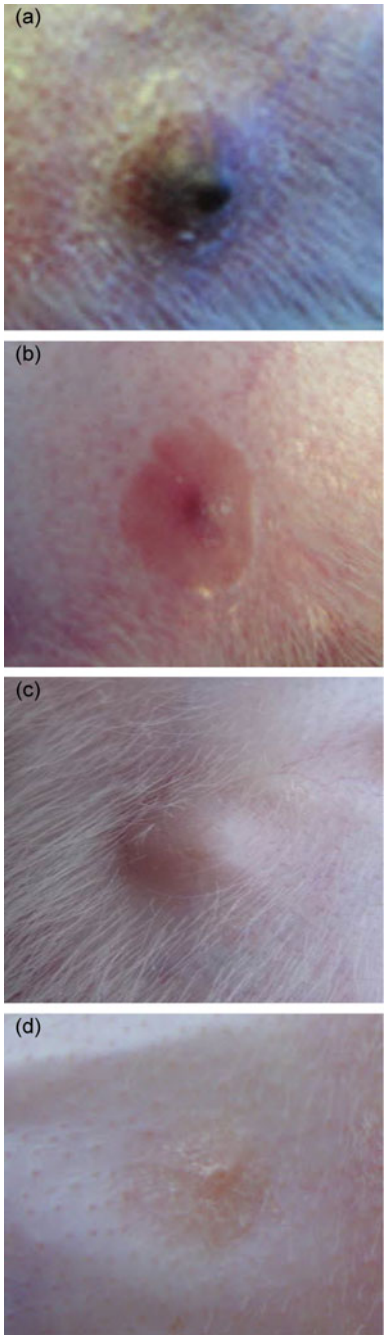

Fig. 1 Macroscopic views of scar samples
(a) Control group (Day 21); (b) Intervention group (Day 21); (c) Control group (Day 35); (d) Intervention group (Day 35)

Table 1 Thickness of scars measured with a slide gauge

Day	Scar thickness (mm)	
	Control group	Intervention group
15	2.45±0.67	2.66±0.55
21	2.31±0.57	2.02±0.38*
28	2.28±0.38	2.11±0.40
35	2.12±0.40	1.71±0.35*

* $p<0.05$, compared to the control group

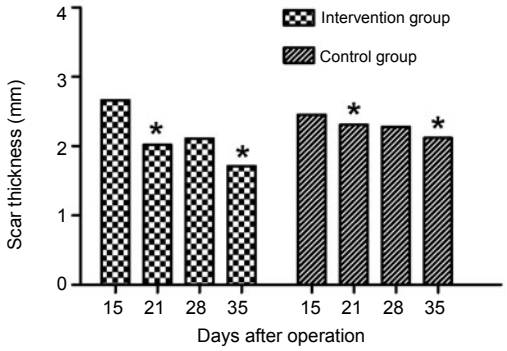

Fig. 2 Comparison of scar thickness
Scar thickness decreased much faster in the intervention group, and significant statistical differences were observed on Days 21 and 35 after modeling (* $p<0.05$)

between the two groups (Table 1 and Fig. 2). After that, the thickness of scars in both groups decreased with time. However, the decrease was much faster in the intervention group than in the control group, and significant statistical differences were observed on Days 21 and 35 after modeling ($p<0.05$).

3.3 Perfusion of microcirculation

The scar microcirculatory perfusion was assessed by laser Doppler flowmetry (Fig. 3).

After healing, the microcirculation perfusion in the control group went up on Day 21 and decreased slowly thereafter, but in the intervention group it continued to drop after endostatin administration. A significant difference between the two groups was observed on Day 21 ($p<0.05$).

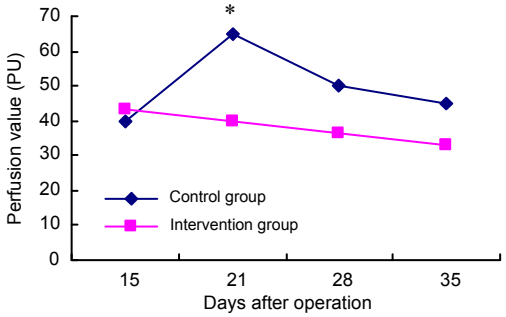

Fig. 3 Changes in microcirculation perfusion in scars
* $p<0.05$, significant difference between the intervention and control groups on Day 21

3.4 SEI

On Day 35 post wounding, the scars were harvested for SEI measurement (Fig. 4).

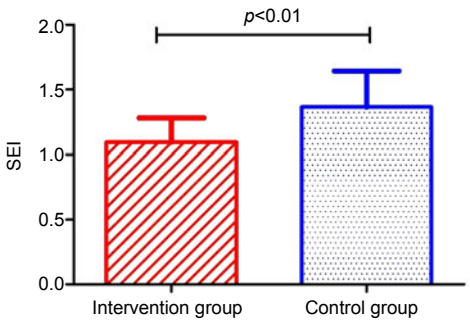

Fig. 4 Comparison of scar elevation index on Day 35

The SEI in the control group was 1.36±0.28, compared to 1.09±0.19 in the intervention group. The difference was statistically significant (p<0.01).

3.5 MVD

MVD within scar samples was measured by specific immunochemical staining of endothelial cells ($CD34^+$). In each scar, the total number of CD34 positive blood vessels was counted in five randomly chosen high power fields, which were distributed evenly inside the scar. The counts from the five fields (200×) were averaged and used for comparisons (Fig. 5).

The MVD in the control group (5.63±1.78) (Fig. 5a) was much higher than that of the intervention group (1.73±0.94) (Fig. 5b) on Day 35. The difference was statistically significant (p<0.05).

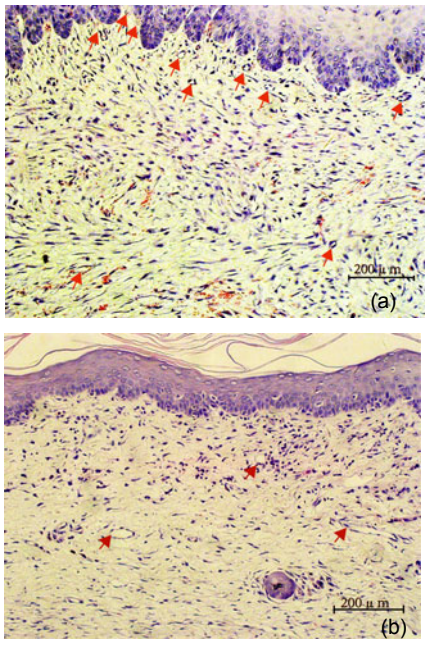

Fig. 5 Microvessel density (MVD) within scar samples
(a) Control group; (b) Intervention group (immunohistochemistry)

3.6 Collagen distribution in scars

Collagen distribution in scar samples, harvested on Day 35 post wounding, was observed by Masson trichrome-stained slides (Fig. 6).

The distribution of collagen fibers in the intervention group in Masson trichrome-stained slides showed regular alignment (Fig. 6b), while fibers were enlarged and disordered in the control group (Fig. 6a).

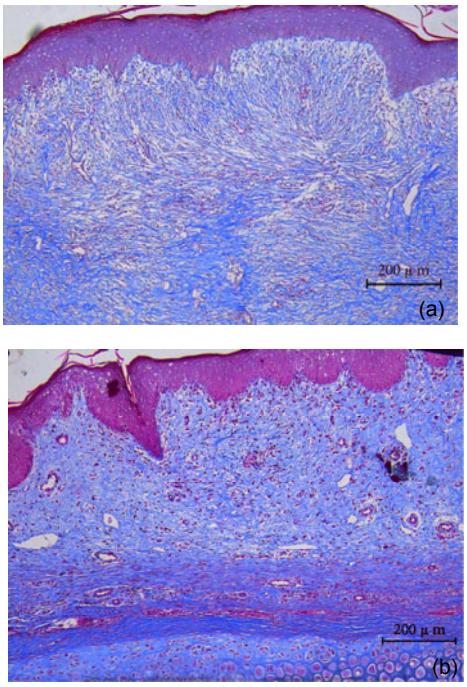

Fig. 6 Collagen distribution in scars on Day 35
(a) Control group; (b) Intervention group (Masson)

3.7 Expressions of type I collagen and Bcl-2 in scars

Expressions of type I collagen and Bcl-2 in scars were measured by Western blot analysis (Fig. 7).

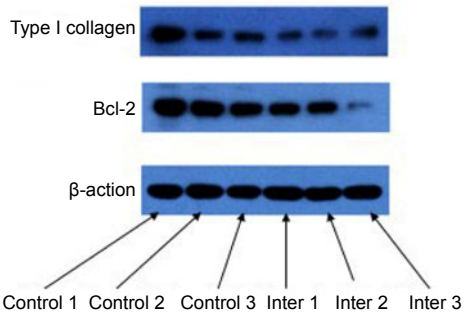

Fig. 7 Expressions of type I collagen and Bcl-2 in scars

Expressions of type I collagen and Bcl-2 were depressed by endostatin injection. Down-regulation of Bcl-2 was possibly related to the apoptosis of endothelium cells.

4 Discussion

Hypertrophic scarring is a common problem after injury and may cause functional and cosmetic deformities. Several treatment modalities have been applied for the prevention and treatment of HS, including pressure, silicone gel sheets, intralesional steroids, 5-fluorouracil (5-FU), cryotherapy, surgical excision, and lasers. Local pharmacological therapies such as repeat inter scar steroid injections, are painful and can result in complications including steroid atrophy. Systemic pharmacologic inhibitors of collagen synthesis such as penicillamine were previously used clinically for these lesions. However, significant systemic side effects of this therapy were reported (Camus and Koeger, 1986). Currently, there is a demand for systemically applied agent collagen synthesis inhibitors, which are considered an attractive strategy if they can be applied without obvious side effects.

Endostatin was first identified from murine hemangioendothelioma cell culture medium (O'Reilly *et al.*, 1997). It has been systemically implicated in tumor therapy by reducing the number of newly-formed blood vessels (Rosca *et al*., 2011). Results from these clinical studies have proven the safety of this drug. Local injection of the anti-angiogenesis drug endostatin has been shown to significantly alleviate scar formation in rabbit ears (Wang *et al*., 2012). However, repeated local injections in the scar are painful for human patients, and lead to poor compliance.

This study, to our knowledge, is the first to confirm the hypothesis that systemic application of endostatin can also be effective in preventing and/or treating local HSs. Our results showed that the systematic injection of endostatin reduced scar congestion, thickness, SEI, and MVD significantly and produced fewer and regular collagen fibers compared to the control group. The effectiveness of endostatin in reducing the thickness and SEI of scars is possibly due to its ability to impede angiogenesis.

The relationships between the endothelial cells and other cells were described previously (Bao *et al*., 2009). The capillary endothelial cells can secrete fibroblast growth factor (FGF) and platelet-derived growth factor (PDGF) which will lead to fibroblast hyperplasia (Bao *et al*., 2009). Bcl-2 is an anti-apoptotic molecule (Portt *et al*., 2011). A decrease in Bcl-2 would promote apoptosis in mammalian cells by directly activating the mitochondrial apoptotic pathway upstream of caspase-9, and caspase-9 naturally activates caspase-3 (Miller, 1997; Fan *et al.*, 2005; Mazars *et al.*, 2005). In the present study, Bcl-2 decreased following endostatin treatment. Thus, the decrease in Bcl-2 played an important role in the induction of endothelial cell apoptosis by endostatin. Our results indicated that endostatin may promote the apoptosis of endothelial cells and block their release of PDGF and FGF, thereby controlling the production of collagen by fibroblasts. Further research should be done to elucidate the mechanism of this process.

5 Conclusions

Our study demonstrates that the inhibition of angiogenesis by endostatin results in an obvious reduction of hypertrophic scarring in a rabbit ear model. To the best of our knowledge, this is the first report of the systemic application of endostatin for targeting the growth of new blood vessels to control local HS formation. By systematic application of endostatin, the inhibition of angiogenesis provides a potential approach for the prevention and treatment of HSs in humans.

References

Amadeu, T., Braune, A., Mandarim-de-Lacerda, C., Porto, L.C., Desmouliere, A., Costa, A., 2003. Vascularization pattern in hypertrophic scars and keloids: a stereological analysis. *Pathol. Res. Pract.*, **199**(7):469-473. [doi:10.1078/0344-0338-00447]

Bao, P., Kodra, A., Tomic-Canic, M., Golinko, M.S., Ehrlich, H.P., Brem, H., 2009. The role of vascular endothelial growth factor in wound healing. *J. Surg. Res*., **153**(2): 347-358. [doi:10.1016/j.jss.2008.04.023]

Camus, J.P., Koeger, A.C., 1986. D-penicillamine and collagen. *Ann. Biol. Clin. (Paris)*, **44**(3):296-299.

Ehrlich, H.P., Kelley, S.F., 1992. Hypertrophic scar: an interruption in the remodeling of repair—a laser doppler blood flow study. *Plast. Reconstr. Surg*., **90**(6):

993-998. [doi:10.1097/00006534-199212000-00009]

Fan, T.J., Han, L.H., Cong, R.S., Liang, J., 2005. Caspase family proteases and apoptosis. *Acta Biochim. Biophys. Sin.*, **37**(11):719-727. [doi:10.1111/j.1745-7270.2005.00108.x]

Kim, Y.S., Jung, D.H., Kim, N.H., Lee, Y.M., Jang, D.S., Song, G.Y., Kim, J.S., 2007. KIOM-79 inhibits high glucose or AGEs-induced VEGF expression in human retinal pigment epithelial cells. *J. Ethnopharmacol.*, **112**(1): 166-172. [doi:10.1016/j.jep.2007.02.017]

Kim, Y.S., Kim, J., Kim, C.S., Sohn, E.J., Lee, Y.M., Jeong, I.H., Kim, H., Jang, D.S., Kim, J.S., 2011. KIOM-79, an inhibitor of AGEs-protein cross-linking, prevents progression of nephropathy in zucker diabetic fatty rats. *Evid. Based Compl. Altern. Med.*, **2011**:761859. [doi:10.1093/ecam/nep078]

Kirsner, R.S., Eaglstein, W.H., 1993. The wound healing process. *Dermatol. Clin.*, **11**(4):629-640.

Kischer, C.W., 1992. The microvessels in hypertrophic scars, keloids and related lesions: a review. *J. Submicrosc. Cytol. Pathol.*, **24**(2):281-296.

Leventhal, D., Furr, M., Reiter, D., 2006. Treatment of keloids and hypertrophic scars: a meta-analysis and review of the literature. *Arch. Fac. Plast. Surg.*, **8**(6):362-368. [doi:10.1001/archfaci.8.6.362]

Marcus, J.R., Tyrone, J.W., Bonomo, S., Xia, Y., Mustoe, T.A., 2000. Cellular mechanisms for diminished scarring with aging. *Plast. Reconstr. Surg.*, **105**(5):1591-1599. [doi:10.1097/00006534-200004050-00001]

Mazars, A., Geneste, O., Hickman, J., 2005. The bcl-2 family of proteins as drug targets. *J. Soc. Biol.*, **199**(3):253 (in French). [doi:10.1051/jbio:2005027]

Miller, D.K., 1997. The role of the caspase family of cysteine proteases in apoptosis. *Semin. Immunol.*, **9**(1):35-49. [doi:10.1006/smim.1996.0058]

Morris, D., Wu, L., Zhao, L., Bolton, L., Roth, S., Ladin, D., Mustoe, T., 1997. Acute and chronic animal models for excessive dermal scarring: quantitative studies. *Plast. Reconstr. Surg.*, **100**(3):674. [doi:10.1097/00006534-199709000-00021]

O'Reilly, M.S., Boehm, T., Shing, Y., Fukai, N., Vasios, G., Lane, W.S., Flynn, E., Birkhead, J.R., Olsen, B.R., Folkman, J., 1997. Endostatin: an endogenous inhibitor of angiogenesis and tumor growth. *Cell*, **88**(2):277-285. [doi:10.1016/S0092-8674(00)81848-6]

Portt, L., Norman, G., Clapp, C., Greenwood, M., Greenwood, M.T., 2011. Anti-apoptosis and cell survival: a review. *Biochim. Biophys. Acta*, **1813**(1):238-259. [doi:10.1016/j.bbamcr.2010.10.010]

Rosca, E.V., Koskimaki, J.E., Rivera, C.G., Pandey, N.B., Tamiz, A.P., Popel, A.S., 2011. Anti-angiogenic peptides for cancer therapeutics. *Curr. Pharm. Biotechnol.*, **12**(8):1101-1016. [doi:10.2174/138920111796117300]

Saulis, A.S., Mogford, J.H., Mustoe, T.A., 2002a. Effect of mederma on hypertrophic scarring in the rabbit ear model. *Plast. Reconstr. Surg.*, **110**(1):177-183, discussion 184-186. [doi:10.1097/00006534-200207000-00029]

Saulis, A.S., Chao, J.D., Telser, A., Mogford, J.E., Mustoe, T.A., 2002b. Silicone occlusive treatment of hypertrophic scar in the rabbit model. *Aesthet. Surg. J.*, **22**(2):147-153. [doi:10.1067/maj.2002.123023]

Song, B., Lu, K., Zhang, Y., Guo, S., Han, Y., Ma, F., Li, H., 2008a. Angiogenesis in hypertrophic scar of rabbit ears and effect of extracellular protein with metalloprotease and thrombospondin 1 domains on hypertrophic scar. *Chin. J. Repar. Reconstr. Surg.*, **22**(1):70-74.

Song, B.Q., Lu, K.H., Guo, S.Z., Zhang, Y., Peng, P., Ma, F.C., Li, H.Y., 2008b. Effect of *METH1* gene transfection on the proliferation of rabbit's ear scar. *Chin. J. Plast. Surg.*, **24**(2):148-150 (in Chinese).

Song, B., Zhang, W., Guo, S., Han, Y., Zhang, Y., Ma, F., Zhang, L., Lu, K., 2009. Adenovirus-mediated *METH1* gene expression inhibits hypertrophic scarring in a rabbit ear model. *Wound Repair Regen.*, **17**(4):559-568. [doi:10.1111/j.1524-475X.2009.00514.x]

Tandara, A.A., Mustoe, T.A., 2008. The role of the epidermis in the control of scarring: evidence for mechanism of action for silicone gel. *J. Plast. Reconstr. Aesthet. Surg.*, **61**(10):1219-1225. [doi:10.1016/j.bjps.2008.03.022]

Thomas, D.W., Hopkinson, I., Harding, K.G., Shepherd, J.P., 1994. The pathogenesis of hypertrophic/keloid scarring. *Int. J. Oral Maxillof. Surg.*, **23**(4):232-236. [doi:10.1016/S0901-5027(05)80377-7]

Wang, Z.Y., Fei, S., Lianju, X., Yingkai, L., Chun, Q., Shuliang, L., Xiqiao, W., 2012. Endostar injection inhibits rabbit ear hypertrophic scar formation. *Int. J. Low Extrem. Wounds*, **11**(4):271-276. [doi:10.1177/1534734612463698]

Zheng, M.J., 2009. Endostatin derivative angiogenesis inhibitors. *Chin. Med. J. (Engl.)*, **122**(16):1947-1951.